

Online Research @ Cardiff

This is an Open Access document downloaded from ORCA, Cardiff University's institutional repository: <https://orca.cardiff.ac.uk/id/eprint/151268/>

This is the author's version of a work that was submitted to / accepted for publication.

Citation for final published version:

Li, Chuanyue, Dong, Xue, Cipcigan, Liana M. ORCID: <https://orcid.org/0000-0002-5015-3334>, Haddad, Abderrahmane ORCID: <https://orcid.org/0000-0003-4153-6146>, Sun, Mingyu, Liang, Jun ORCID: <https://orcid.org/0000-0001-7511-449X> and Ming, Wenlong ORCID: <https://orcid.org/0000-0003-1780-7292>
2022. Economic viability of dynamic wireless charging technology for private EVs. IEEE Transactions on Transportation Electrification
10.1109/TTE.2022.3163823 file

Publishers page: <http://dx.doi.org/10.1109/TTE.2022.3163823>
< <http://dx.doi.org/10.1109/TTE.2022.3163823> >

Please note:

Changes made as a result of publishing processes such as copy-editing, formatting and page numbers may not be reflected in this version. For the definitive version of this publication, please refer to the published source. You are advised to consult the publisher's version if you wish to cite this paper.

This version is being made available in accordance with publisher policies.

See

<http://orca.cf.ac.uk/policies.html> for usage policies. Copyright and moral rights for publications made available in ORCA are retained by the copyright holders.



Economic viability of dynamic wireless charging technology for private EVs

Chuan Yue Li, *Member, IEEE*, Xue Dong, Liana M. Cipcigan, *Member, IEEE*,
Abderrahmane Haddad, *Member, IEEE*, Mingyu Sun, *Member, IEEE*, Jun Liang, *Senior Member, IEEE*,
Wenlong Ming, *Member, IEEE*

Abstract—Dynamic wireless charging (DWC), which enables charging while EVs are in motion, is an attractive charging way. However, additional installed power tracks underneath the lane bring a significant concern on its economic viability. This paper proposes a comprehensive framework to evaluate the economic viability of the DWC lane for private EVs. The investment of local power support with renewable energy integration and energy storage is also considered in the DWC system. Charging choices of private EVs among multiple charging providers are modelled to estimate the electricity demand of the DWC system. The grid impact of the DWC system is studied via a multi-bus AC network. Moreover, an optimization policy is proposed to maximize the DWC provider's profit and minimize the grid impact by adjusting the charging price and electricity procurement at each horizon. It is found that the payback period of the DWC system with the proposed optimization policy is shortened by 25% compared with the fixed charging price strategy. Even with a tight grid impact limit, the payback period will not be significantly longer under the proposed optimization policy. When the efficiency of the DWC lane increases to 90% and the cost reduces to 50%, the payback period is shortened by 19% and 22%, respectively.

Index Terms—Electric vehicle, dynamic wireless charging, renewable energy, energy storage, multi-objective optimization

I. INTRODUCTION

DECARBONIZING transportation is crucial to mitigate climate change. The sale of fuel-powered vehicles will be banned in many countries from 2040 [1], and the accelerated introduction of electric vehicles (EVs) by automakers is an observable trend. The EV adoption rate highly depends on the large-scale deployment of charging infrastructure and desired charging speed. The current plug-in charging method has two main inherent disadvantages: the limited per-charging distance and the unavailable moving during charging. To increase the range, EVs are required to either install a larger size of battery or stop for being charged frequently.

The dynamic wireless charging (DWC), which enables charging while the EVs are in motion, can become a potential alternative method without the aforementioned drawbacks associated with the plug-in charging method. In the DWC

system, the energy from the power track embedded under the road's surface is wirelessly transferred to the receivers fitted in moving vehicles. A large amount of EVs could be charged at the same time when they travel over the DWC road. For constant-route EVs, DWC can be a more cost-effective approach than increasing battery capacity in terms of extending range [2]. In comparison with stationary charging, DWC is found to be more attractive to the EV drivers even at a 115% charging price [3]. To achieve long air-gap and high-power transmission, inductive power transfer technology is used for the DWC [4]. Besides, power track designs, vehicle position detections, and power transfer enhancements have been progressing fast in recent years. Two types of power tracks have been advised: the lumped track [5] and the stretched track [6]. A lumped track [7] is made of a string of coils, whose dimension is similar to the receiver coil. To simplify the construction and increase the tolerance of lateral displacement, a thin stretched track [8] is designed to be much longer than the receiver coil. The vehicle position detection using the principle of inductive magnetic coupling is proposed to avoid EV misalignment [9] and unnecessary switched-on power tracks [10]. Therefore, a stable dynamic wireless power transfer is maintained at the desired power level and unnecessary power loss is avoided. To improve the efficiency of dynamic wireless power transfer, compensation circuits are designed based on LCC circuit [11], which can also stabilize the power transfer against the coupling variance during dynamic charging [12].

To propel the feasibility of EV using DWC technology, many technical efforts have been progressing fast for long air-gap and high-power transmission, EV misalignment correction, and high power transfer efficiency. Inductive wireless power transfer technology has been validated widely for this long air-gap and high-power transmission. Two types of power tracks using inductive wireless power transfer technology [4], which are lumped track [5] and stretched track [6] have been developed and validated for EVs being charged dynamically at a practical air-gap such as 15 cm. A lumped track [7] is made of a string of coils, whose dimension is similar to the receiver coil. To simplify the construction and increase the tolerance of lateral displacement, a thin stretched track [8] is designed to be much longer than the receiver coil. The vehicle position detection using the principle of inductive magnetic coupling is proposed to avoid EV misalignment [9] and unnecessary switched-on power tracks [10]. Therefore, a stable dynamic wireless power transfer is maintained at the desired power

We are grateful for support from the Decarbonising Transport through Electrification (DTE) Network+ funded by EPSRC grant reference EP/S032053/1 and UK National Grid Electricity Transmission under grant NIA NGT0001.

C. Li, L. M. Cipcigan, A. Haddad, J. Liang and W. Ming are with Cardiff University, Cardiff, CF24 3AA, U.K.

M. Sun is with National Grid Electricity Transmission, Warwick, CV34 6DA, U.K.

X. Dong is with Zhejiang University of Finance and Economics, Hangzhou, China. (*corresponding author*: Xue Dong, xue.dong6@outlook.com)

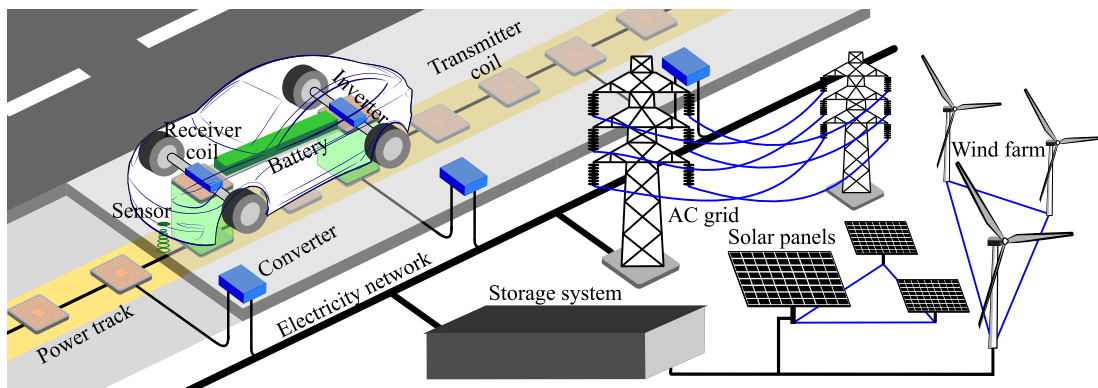


Fig. 1. Dynamic wireless charging system with renewable integration and storage system.

level and the unnecessary power loss is saved. To enhance the efficiency of dynamic wireless power transfer, compensation circuits are designed based on LCC circuit [11], which can also stabilize the power transfer against the coupling variance during dynamic charging [12].

The aforementioned technical advance propels the industrial development of EVs adopting DWC. Many EVs using DWC have been demonstrated by labs, projects and companies [13] [14] [15], including KAIST, ORNL, VICTORIA project, FABRIC project, Bombardier, INTIS, and Qualcomm. Tesla also patented [16] its wireless onboard chargers, which enable its EVs to be charged wirelessly. The details of these DWC prototypes are summarized in Table I. The validation of technical feasibility via prototypes has brought a big step for DWC towards commercialized EV charging.

Besides technical aspects, economic viability is also of great importance to the commercialization of DWC for EVs. The initial investment on extensively deployed power tracks embedded under roads brings concern about its economic viability. Public-private partnership is explored to promote the development of this DWC system. It is found that the 15-year concession period with a 12.5% return rate for private investors would be an attractive way [17]. To minimize the infrastructure cost, optimization via a generic method for the DWC lane between its length reduction and power level increase is conducted, which reduced the costs by 34% [18]. To compensate the additional cost of DWC tracks, the position of the DWC lane and EV battery size are optimized via the particle swarm optimization method or the generic method. As a result, the size of EV battery has been reduced by 40% [19] [20]. In comparison with conventional stationary charging, DWC can be more economic with a 20% total cost reduction by the optimization between the length of power tracks and total reduction of EV battery size [21]. Furthermore, optimized deployment of multiple DWC routes has been discussed via the particle swarm optimization method to minimize the investment cost of DWCs [22].

However, the aforementioned economic analysis methods simplify the EV charging choice and only consider constant-route EVs. The attraction for EVs among different charging stations and different charging technologies are yet to be considered. Furthermore, power support limitation of the grid

and investment of local renewable energy and storage are not included in the economic analysis either.

To fill the gap above, this paper proposes a comprehensive framework to evaluate the economic viability of the DWC system for private EVs. This DWC lane with tens of kilometer length works as a charging station with integration of local renewable energy and storage system. Its profit comes from the payment of EV charging. Accommodating a large amount of EVs for charging results in a heavy load on the grid. Therefore, EV charging management of DWC is considered to avoid the immoderate impact on the grid. On the other hand, the impact of grid power support limitation on the profit of DWC is evaluated. Moreover, the investment of local renewable energy and storage systems, which help to power the DWC lane, is included in the economic analysis. The main technical contributions of this paper are as follows:

- a multi-objective and multi-horizon optimization policy is proposed to guide the DWC provider to set charging prices and manage electricity procurement by jointly maximizing the profit of the DWC providers and minimizing the grid impact.
- electricity demand of the DWC is modelled based on EV choices among different charging providers. To quantify the EV choice comprehensively, the following factors are considered: charging speed, charging price, and travel time to charging providers.
- the guidance of DWC electricity procurement is proposed to avoid the immoderate grid voltage variance; this grid impact of the DWC is assessed using power flow analysis with multiple constraints including power flow and line losses.

The paper is organised as follows. In section II, the model for the DWC system is developed, which includes DWC technology, storage system, renewable energy generation, profit of the DWC, and grid impact. Section III quantifies the EV charging choice among different charging methods at different locations, which helps to derive the charging demand of DWC. In section IV, an optimization policy is proposed for the DWC provider to maximize the profit and minimize the grid impact. Case studies are conducted in Section V to show the effectiveness of aforementioned DWC system modelling, and analyze the economic viability of this DWC system. In section

TABLE I
DEMONSTRATIONS OF DYNAMIC WIRELESS CHARGING [13] [14] [15]

Organization	Power (kW)	Efficiency (%)	Airgap (cm)	Converter's operation frequency (kHz)
KAIST	22	71	20	20
ORNL	2.2	74	10	22
VICTORIA project	50	83	-	-
FEBRIC project	up to 200	70-80	-	20-85
Bombardier	up to 200	-	-	-
INTS	60	-	15	35
	30	-	15	35
Qualcomm Halo	20	80	-	85

Note: "-" means the value is not reported.

IV, we summarize the models and economic analysis.

II. FORMULATION FOR DYNAMIC WIRELESS CHARGING SYSTEM

Comparing to the urban area, EVs on the highway, which have less traffic fluctuation and relatively stable moving speed, are reported [23] to be more suitable for DWC. DWC system, which requires power tracks to be installed underneath one lane of the highway, is considered in our study, as shown in Fig. 1. Any EVs of this highway can be driven on the DWC lane for charging. Large-scale EV charging dynamically on the lane presents a substantial load, which is powered by the AC grid and renewable integration. For avoiding intermittence of the renewable sources, their generation is collected in the storage system first. At the same time, the storage system also can procure electricity from the AC grid if necessary. Therefore, the DWC lane is supplied by both the local storage system and the AC grid. The charging provider makes a profit from revenue of DWC and investigates the DWC lane, storage, and renewable energy generator.

Formulation of the DWC system, as shown in Fig. 1, is carried out in each planning horizon as five parts including the electricity demand of DWC, Storage, Renewable generation, profit and grid impact.

A. Dynamic wireless charging technology

For a moving vehicle on the DWC lane, the electricity is transferred between receiver coils and transmitter coils wirelessly based on inductive coupling, as shown in Fig. 1. Receivers are installed on the EV with an onboard inverter, which conducts AC/DC conversion to charge the onboard battery. Power tracks made of transmitter coils are laid under the DWC lane. For efficient inductive coupling, the track is powered by the current with tens of kHz [14] via road-side converters. Each road-side converter in Fig. 1 represents a combination of power electronic converters as an asynchronous interface between the electricity network and the power track.

A sensor for position detection is installed on the EV to drive the EV just above the power track, as shown in Fig. 1. However, EVs in motion cannot retain the strongest inductive coupling during the EVs move to the next transmitter coil, which results in the reduction of wireless power transfer efficiency. Normally, the efficiency of static wireless power transfer can reach over 95% [24], while the dynamic wireless power transfer's efficiency is reduced to 70-80%. During k -th

horizon, electricity demand (d_k^{dwc}) of the DWC lane is given below:

$$d_k^{dwc} = \frac{d_k^{ev}}{\eta_{dwc}}, \quad (1)$$

where d_k^{ev} is the charging demand of EVs using DWC, η_{dwc} is the power transfer efficiency of the DWC.

For EVs with charging requirements on the highway, DWC is not their only option. There are many other charging technologies under different charging speeds available. The estimation of d_k^{ev} using DWC is complex and will be formulated clearly in Section III.

B. Electricity exchange of storage system

Services of the storage are normally classified in three categories [25], including energy support, frequency, and voltage regulation. In our study, the energy support for the DWC is considered. The storage is charged from the renewable energy source and electricity procurement with the AC grid. Therefore, the electricity exchange within the storage are given below:

$$E_{k+1} = E_k + \eta_s d_k^{grid} + \eta_s g_k^{ren} - \frac{d_k^{dwc}}{\eta'_s} + \varepsilon_k^e, \quad (2)$$

$$\text{s.t. } SOC_{min} < E_{k+1} < SOC_{max}, \quad (2a)$$

$$-P_s^{max,dis} < (\eta_s d_k^{grid} + \eta_s g_k^{ren} - \frac{d_k^{dwc}}{\eta'_s})/T < P_s^{max,cha}, \quad (2b)$$

where E_k is the stored electricity at the beginning of k -th horizon; d_k^{grid} and g_k^{ren} are respectively electricity procurement from the grid and renewable generation, their power transfer efficiencies are η_s ; η'_s is the power transfer efficiency from the storage to the grid; besides, ε_k^e is the process noise of the energy storage, which follows the Gaussian distribution with zero mean and variance σ^e ; $P_s^{max,cha}$ and $P_s^{max,dis}$ are respectively maximum charging and discharging rate of the storage; T is the period of one horizon.

The state of charge limitation is imposed to avoid the fast storage cycle degradation [26], which is shown on (2a). The charging/discharging speed of the storage is another constraint to limit the power exchange within the storage, which is given as (2b).

C. Renewable energy generation

The generation profile of renewable energy is developed to fulfil the demand of DWC along with the electricity procurement from the grid. Compared to the Monte Carlo approach or generation prediction based on monitoring real data, the statistical method using Markov chain [27], which is based on historical data, is an effective way at the planning stage to describe the random behaviour of solar generation. Thus, the renewable energy generation g_{k+1}^{ren} at next horizon is estimated by a transition matrix \mathbf{TM} of the Markov chain and the generation at k -th horizon. The transition matrix is estimated based on the massive historical data. Suppose there are S possible states of renewable energy generation at each

horizon, these S generation states are represented by matrix \mathbf{g}_k^{ren} . The dimension of the transition matrix is $S \times S$. The transition matrix at the k -th horizon is given by:

$$\mathbf{TM}_k = \begin{bmatrix} P_{k,1,1} & P_{k,1,2} & \dots & P_{k,1,S} \\ P_{k,2,1} & P_{k,2,2} & \dots & P_{k,2,S} \\ \vdots & \vdots & \ddots & \vdots \\ P_{k,S,1} & P_{k,S,2} & \dots & P_{k,S,S} \end{bmatrix}, \quad (3)$$

where $P_{k,s,s}$ is the transition probability of renewable energy between adjacent states at k -th horizon.

The generation states \mathbf{g}_{k+1}^{ren} at $(k+1)$ -th horizon can be estimated in the next iteration:

$$\mathbf{g}_{k+1}^{ren} = \mathbf{TM}_k \times \mathbf{g}_k^{ren}. \quad (4)$$

The generation at k -th horizon \mathbf{g}_k^{ren} is calculation based on the expectation value of generation states, as shown below:

$$\mathbf{g}_k^{ren} = \mathbb{E}(\mathbf{g}_k^{ren}). \quad (5)$$

D. Profit of dynamic wireless charging provider

The profit made by the DWC lane at each horizon is formulated for economic analysis. Charging prices p_k^{dwc} is updated at the start of each horizon. After considering the maintenance cost at each horizon of the dynamic charging infrastructure, storage and the renewable source, the profit (Π_k) of the k -th horizon is therefore calculated as:

$$\Pi_k = p_k^{dwc} d_k^{ev} - p_k^{grid} d_k^{grid} - C_s(E_k + \eta_s d_k^{grid} + \eta_s g_k^{ren} - \frac{d_k^{dwc}}{\eta'_s} + \varepsilon_k^e), \quad (6)$$

where d_k^{grid} is the electricity procurement from the grid, p_k^{grid} is the day-ahead market price of the electricity procurement from the grid, C_s is the maintenance cost per MWh.

The total capital cost includes initial investment of DWC tracks, renewable energy infrastructure and storage system, which is calculated as below:

$$C_{total} = C_{ren} + (C_{dwc}^p + C_{dwc}^c) L_{dwc} + C_{storage} E_{storage}, \quad (7)$$

where C_{total} is the total capital cost, C_{ren} is the cost of renewable energy source, C_{dwc}^p is the cost of DWC power tracks per kilometer, C_{dwc}^c is the cost of construction and maintenance, L_{dwc} is the length of DWC lane, $C_{storage}$ is the cost of storage per kWh, $E_{storage}$ is the total capacity of storage.

The payback period t_{pd} is the time that the cumulated profit just goes over the initial investment, which is presented below:

$$C_{total} = \sum_{k=1}^{t_{pb}} \Pi_k. \quad (8)$$

E. Impact on AC grid

For avoiding an unacceptable impact on the grid, the grid impact is quantified to guide the electricity procurement at each horizon. In our study, the induced voltage variation because of the electricity procurement on each bus of AC

TABLE II
PARAMETERS OF BUSES FOR POWER FLOW CALCULATION

Bus types	Slack	PV	PQ
Number	1	N_{PV}	N_{PQ}
Known parameters	$V \delta$	$P V$	$P Q$
Unknown parameters	$P Q$	δQ	$V \delta$
Number of required equations for each bus	0	1	2

grid is considered as the grid impact. Besides, electricity procurement can be limited by the maximum allowable grid impact.

The voltage variation (magnitude V and phase δ) on each bus in the AC grid, that is induced by the power demand of the DWC, is normally calculated via the power flow analysis. It is assumed that the total number of buses is $1 + N_{PQ} + N_{PV}$ including 1 slack bus, N_{PQ} PQ buses, and N_{PV} PV buses. Unknown V and δ of all buses are summarized into Table II. Therefore, solving all V and δ requires $N_{PQ} + N_{PV}$ active power equations (PV and PQ buses) and N_{PQ} reactive power equations (PQ buses). The active and reactive power equations on each bus are given below:

$$P_i = \sum_{j=i}^N V_i V_j [G_{ij} \cos(\delta_i - \delta_j) + B_{ij} \sin(\delta_i - \delta_j)], \quad (9)$$

$$Q_i = \sum_{j=i}^N V_i V_j [G_{ij} \sin(\delta_i - \delta_j) - B_{ij} \cos(\delta_i - \delta_j)], \quad (10)$$

where P_i (including P_i^{grid}) and Q_i are respectively the net active and reactive power injected at bus i ; G_{ij} and B_{ij} are respectively conductance and susceptance of the ij -th element of admittance matrix.

These $2N_{PQ} + N_{PV}$ equations are non-linear, as shown in (9)-(10), which brings a great challenge to solve directly. Therefore, the Newton-Raphson approximation method is used to find the voltage variation, as shown below:

$$\begin{bmatrix} \Delta \mathbf{V} \\ \Delta \boldsymbol{\delta} \end{bmatrix} = \underbrace{\begin{bmatrix} \frac{\partial \mathbf{P}}{\partial \boldsymbol{\delta}} & \frac{\partial \mathbf{P}}{\partial \mathbf{V}} \\ \frac{\partial \mathbf{Q}}{\partial \boldsymbol{\delta}} & \frac{\partial \mathbf{Q}}{\partial \mathbf{V}} \end{bmatrix}}_{\mathbf{J}^{-1}} \begin{bmatrix} \Delta \mathbf{P} \\ \Delta \mathbf{Q} \end{bmatrix}, \quad (11)$$

where $\Delta \mathbf{V}$ and $\Delta \boldsymbol{\delta}$ are respectively the voltage vectors of magnitude variation and phase variation. $\Delta \mathbf{P}$ and $\Delta \mathbf{Q}$ are the increased power demand from the DWC system. \mathbf{J} is the Jacobian matrix based on the power equations (9-10), each term is a sub-matrix, as shown below (using $\partial \mathbf{P} / \partial \boldsymbol{\delta}$ as an example):

$$\frac{\partial \mathbf{P}}{\partial \boldsymbol{\delta}} = \begin{bmatrix} \frac{\partial P_1}{\partial \delta_1} & \frac{\partial P_1}{\partial \delta_2} & \dots & \frac{\partial P_1}{\partial \delta_{N_{PQ} + N_{PV}}} \\ \frac{\partial P_2}{\partial \delta_1} & \ddots & & \vdots \\ \vdots & & \ddots & \vdots \\ \frac{\partial P_{N_{PQ} + N_{PV}}}{\partial \delta_1} & \dots & \dots & \frac{\partial P_{N_{PQ} + N_{PV}}}{\partial \delta_{N_{PQ} + N_{PV}}} \end{bmatrix}. \quad (12)$$

The power flow calculation within the grid based on (11) is given below:

$$P_{ij} = \frac{V_i^2 \cos(\phi_{ij}) - V_i V_j \cos(\delta_i - \delta_j + \phi_{ij})}{Z_{ij}}, \quad (13)$$

$$Q_{ij} = \frac{V_i^2 \sin(\phi_{ij}) - V_i V_j \sin(\delta_i - \delta_j + \phi_{ij})}{Z_{ij}}, \quad (14)$$

where P_{ij} and Q_{ij} are respectively the active and reactive power flow on line ij between bus i and bus j . $Z_{ij} \angle \phi_{ij}$ is the line impedance between bus i and bus j .

The power loss on each line is calculated as:

$$P_{ij}^L = \frac{\cos(\phi_{ij})(V_i^2 + V_j^2) - V_i V_j \cos(\delta_i - \delta_j + \phi_{ij})}{Z_{ij}} + \frac{-V_i V_j \cos(\delta_j - \delta_i + \phi_{ij})}{Z_{ij}}, \quad (15)$$

where P_{ij}^L is the power loss on line ij .

We assume that the DWC system connects to the M buses and the electricity procurement from these M buses is formulated as below:

$$d_k^{grid} = T_k \times \sum_i^M (P_i^{grid}), \quad (16)$$

where P_i^{grid} is the procured power at bus i and this P_i^{grid} belongs to P_i , which is the net active power at bus i ; T_k is the period of k -th horizon.

Voltage variation at each bus because of this electricity procurement are calculated based on (11), and their 1-norm value is used to quantify the grid impact Λ_k , as shown below:

$$\min_{d_k^{grid}} \Lambda_k = \left\| \begin{bmatrix} \Delta \mathbf{V} \\ \Delta \delta \end{bmatrix} \right\|_1$$

$$= \left\| \begin{bmatrix} \frac{\partial \mathbf{P}}{\partial \delta} & \frac{\partial \mathbf{P}}{\partial \mathbf{V}} \\ \frac{\partial \mathbf{Q}}{\partial \delta} & \frac{\partial \mathbf{Q}}{\partial \mathbf{V}} \end{bmatrix} \begin{bmatrix} \mathbf{P}_i^{grid}(d_k^{grid}) \\ \Delta \mathbf{Q} \end{bmatrix} \right\|_1, \quad (17)$$

$$\text{s.t. } \Lambda_k < \Lambda_{max}, \quad (17a)$$

$$-P_{ij}^{max} < P_{ij} < P_{ij}^{max}, \quad (17b)$$

$$-Q_{ij}^{max} < Q_{ij} < Q_{ij}^{max}, \quad (17c)$$

$$P_{ij}^L < P_{ij}^{L,max}. \quad (17d)$$

The objective function (17) indicates the grid impact caused by the power procurement from the DWC system. The voltage and power constraints are imposed to ensure the healthy operation of the connected grid. Constraint (17a) limits the voltage variance in an acceptable range. Power constraints (17b-17d) guarantee the power flow and losses on each line are within a safe range.

III. CHARGING DEMAND ESTIMATION OF EVs USING DYNAMIC WIRELESS CHARGING SYSTEM

There are other charging methods, such as conductive charging, supported by various providers rather than the DWC provider. And charging providers can be located in different areas. In this section, the choice model is proposed to estimate

the number of EVs that choose the DWC provider rather than other charging providers.

We assume that the n -th EV's charging demand d_n^{ev} is a random variable uniformly distributed in the range $[D_l, D_u]$, where D_l and D_u are the lower and upper limit of charging demand respectively. The EV charging demand of s -th charging provider at k -th horizon is estimated as:

$$d_k^{ev,s} = \sum_{n \in N} d_n^{ev} P_n^s, \quad (18)$$

where N is the total number of EVs that require charging; P_n^s is the possibility that n -th EV selects s -th charging provider; N denotes the total number of EVs.

A. Choice modeling of EV charging providers

For quantifying the choice, the probability of charging on the DWC lane is estimated by logit model [27], which is widely used in the analysis and prediction of a consumer's choice from a finite set of choice alternatives. The choice may be influenced by many factors [28] such as charging price, charging time, EV owner's income, travel time to charging stations, convenience for charging, etc. In our study, travel time, charging price, and charging speed are accounted for the choice model to estimate the EV charging demand for the DWC provider. The utility that n -th EV owner obtains from s -th charging provider is decomposed as:

$$U_n^s = u_n^s + \varepsilon_n^s \quad (19)$$

where u_n^s is the known utility and ε_n^s is the unknown utility.

For defining the observable utility, we assume that the differences among charging providers include travel time, charging price and charging time. Therefore, the observable utility is given below:

$$u_n^s = \beta_0^s - \beta_1 t^{rs} - \beta_2 (p^s)^2 + \alpha_1 (1 - e^{-\frac{\alpha_2}{t^s}}) \quad (20)$$

where tt^{rs} represents the travel time from origin point to the charging provider. t^s and p^s represent the charging time and the retail charging price of s -th charging provider respectively; shorter charging time implies better charging service experience and higher utility; a higher retail charging price and longer travel time result in less utility.

The logit model is obtained by assuming that each ε_n^s is independently, identically distributed extreme value. The density for each unobserved component of utility is given below:

$$f(\varepsilon_n^s) = e^{-\varepsilon_n^s} e^{-e^{-\varepsilon_n^s}}. \quad (21)$$

The cumulative distribution is:

$$F(\varepsilon_n^s) = e^{-e^{-\varepsilon_n^s}}. \quad (22)$$

The EV owner will pick the s -th charging provider which brings the maximum utility. The logit choice probabilities for picking s -th charging provider is presented as:

$$P_n^s = \text{Prob}(U_n^s > U_n^j, \forall s \neq j),$$

$$= \text{Prob}(\varepsilon_n^j < u_n^s + \varepsilon_n^s - u_n^j, \forall s \neq j), \quad (23)$$

where $j \in S$ and it represents the j -th charging provider.

According to (22), P_n^s is the cumulative distribution for each ε_n^j evaluated at $u_n^s + \varepsilon_n^s - u_n^j$. Since each ε_n^j is independent, this cumulative distribution over all $s \neq j$ is the product of the individual cumulative distributions, which is given below:

$$P_n^s | \varepsilon_n^s = \prod_{j \neq s} e^{-e^{-(u_n^s + \varepsilon_n^s - u_n^j)}}. \quad (24)$$

ε_n^s is unknown, and the choice probability is the integral of $P_n^s | \varepsilon_n^s$ over all values of ε_n^s in (21), which is given below:

$$\begin{aligned} P_n^s &= \int \left(\prod_{j \neq s} e^{-e^{-(u_n^s + \varepsilon_n^s - u_n^j)}} \right) e^{-\varepsilon_n^s} e^{-e^{-\varepsilon_n^s}} d\varepsilon_n^s \\ &= \int \exp \left(-e^{\varepsilon_n^s} \sum_j e^{-(u_n^s - u_n^j)} \right) e^{-\varepsilon_n^s} d\varepsilon_n^s. \end{aligned} \quad (25)$$

Define $x = e^{-\varepsilon_n^s}$ such that $dx = -e^{-\varepsilon_n^s} d\varepsilon_n^s$, and $\varepsilon_n^s \in (-\infty, \infty)$ results in $x \in (0, \infty)$, (25) is written as:

$$\begin{aligned} P_n^s &= \int_0^\infty \exp \left(-x \sum_j e^{-(u_n^s - u_n^j)} \right) dx \\ &= \frac{\exp(-x \sum_j e^{-(u_n^s - u_n^j)})}{-\sum_j e^{-(u_n^s - u_n^j)}} \Big|_0^\infty. \end{aligned} \quad (26)$$

(26) can be reformulated as a succinct expression:

$$P_n^s = \frac{e^{u_n^s}}{\sum_{j \in S} e^{u_n^j}}. \quad (27)$$

Therefore, the possibility of choosing s -th charging provider is described by (27).

B. Estimation of travel time to EV charging providers

The travel time accounted in utility function (20) is estimated via the combined distribution and assignment model [28]. There are many transportation routes for EVs to travel from their origin nodes to charging providers, the distribution and the assignment of the EV traffic on these links are formulated below:

$$\begin{aligned} \min_{f, q \geq 0} & \sum_{a \in A} \int_0^{\sum_{r \in R} \sum_{s \in S} f_a^{rs}} tt_a(f) df \\ & + \frac{1}{\beta_1} \sum_{r \in R} \sum_{s \in S} q^{rs} (\ln q^{rs} - 1) \\ & + \beta_2 (p^s)^2 - \beta_0^s - \alpha_1 (1 - e^{-\frac{\alpha_2}{\tau^s}}), \end{aligned} \quad (28)$$

$$\text{s.t.} \quad \sum_{a \in A} f_a^{rs} = q^{rs}, \quad (28a)$$

$$\sum q^{rs} = N, \quad (28b)$$

where R is a set of EV origins, indexed by r , S is a set of charging providers (destinations), indexed by s ; $r-s$ routes can be different combination of transportation links A , indexed by a ; q^{rs} represents the total origin-destination flow from r to s , f_a is the traffic flow on link a , tt_a is the travel time of link a .

The objective function (28) is constructed to satisfy the minimum overall travel time on all links and maximum overall EVs' utility [29]. Therefore, EV equilibrium and the multinomial logit destination choice assumption are guaranteed. EV equilibrium requires that travel times in all used $r-s$ routes are equal and less than those that would be experienced by a single vehicle on any unused route. Multinomial logit destination choice assumption requires $q^{rs}/N = P_n^s$. (28a) ensures the EV flow conservation at each node, including the origin and destination nodes; and (28b) restricts the total trips originated from node r to be equal to total number of EVs at that location.

IV. OPTIMIZATION POLICY FOR CHARGING PRICE AND ELECTRICITY PROCUREMENT

At each horizon, charging price and electricity procurement are decided by the DWC provider in order to pursue generous profit and low grid impact. Accordingly, we propose this optimization policy function that incorporates both aims of maximizing its profit and minimizing the grid impact at each horizon, which is given below:

$$\begin{aligned} \mathbf{U}_k &= \max_{\mathbf{X}_k} \{ \mathbb{E}(\Pi_k), \mathbb{E}(-\Lambda_k) \}, \quad (29) \\ \text{s.t.} & \begin{cases} \mathbb{E}(\Pi_k) \geq 0, \\ p_k \geq 0, \\ d_k^{grid} \geq 0, \\ m \leq m_{max}, \\ \Lambda_k \leq \Lambda_{max}, \\ 0 \leq E_k + \eta_s d_k^{grid} + \eta_s g_k^{ren} - \frac{d_k^{dwc}}{\eta_s} + \varepsilon_k^e \leq E, \end{cases} \end{aligned}$$

where $\mathbf{X}_k = [p_k^{dwc}, d_k^{grid}]$ is the vector of decision variables (charging price and grid demand), and $\mathbb{E}(\cdot)$ represents the expectation operation, m_{max} is the maximum number of EVs on DWC lane; profit, charging price and grid demand are required to be positive; number of EVs using DWC and the grid impact are limited within m_{max} and Λ_{max} respectively; electricity transfer in the storage are limited within $[0, E]$, where E is the capacity of storage.

In this policy function, profit Π_k and grid impact Λ_k are defined in Section II (6) and Section III (17). To explain clearly our formulated DWC system, the process flow from charging price and electricity procurement to profit and grid impact is drawn in Fig. 2(a). Basically, the charging price of DWC determines its attractiveness to EVs over other charging providers, and simultaneously affects the charging demand of the DWC service. This charging demand is fulfilled by the electricity from the storage, renewable energy generation, and grid electricity procurement. However, a large amount of electricity procurement will increase grid impacts. Therefore, we solve the optimization problem to obtain the policy function that determines retail DWC price and the appropriate amount of procured electricity at each horizon, in order to maximize the profit and minimize the grid impact. Furthermore, global optimization is also included across multiple horizons.

For global optimization, DWC provider ultimately attempts to maximize his aggregated utility across multiple horizons

subject to several constraints (29) through its decision variables \mathbf{X}_k , which is formulated below:

$$(\mathbf{X}_1^*, \mathbf{X}_2^*, \dots, \mathbf{X}_K^*) = \arg \max_{\mathbf{X}_1, \dots, \mathbf{X}_k} \left\{ \sum_{k=1}^K \mathbf{U}_k \right\}. \quad (30)$$

A multi-objective and multi-horizon optimization, which is formulated by (29) and (30), is required to be solved. For maximizing aggregated utility, dynamic programming as a global optimization algorithm is applied. At each horizon, a multi-objective problem, that is how to optimize the trade-off between two competing objectives of profit and grid impact, is solved by deriving the Pareto frontier of (29). The algorithms for the multi-objective and multi-horizon optimization are explained below.

A. Algorithm for multi-objective optimization at each horizon

The approaches for multi-objective optimization are generally based on two algorithms: scalarizing-based algorithm and evolutionary algorithm. The scalarizing-based algorithm converts multiple objectives into a parametric single-objective function, such as weighted-sum approach and ϵ -constraint approach [30]. Although the conversion simplifies the optimizing process, the distortion may appear in its derived Pareto frontier.

Complete Pareto frontier can be explored based on an efficient and massive search using genetic algorithms, one of which is named non-dominated sorting genetic algorithm II (NSGA II) [31] is used in our study. Elitism is adopted in NSGA II to speed up the convergence process and prevent the loss of good solutions. A sufficient number of generations are generally applied as a termination criterion in order to achieve the full convergence to the Pareto frontier. It is validated that 500 generations [31] [32] are effectively to determine the complete Pareto frontier.

The optimization process of NSGA II is drawn in Fig. 2, the objective function is (29). Firstly, $2N$ population \mathbf{X}_k are generated based on generic algorithm via selection, recombination and mutation. Accordingly, $2N$ \mathbf{U}_k are calculated from (29). After non-dominant and crowding distance sorting, N \mathbf{U}_k are selected. The process will be terminated, if N \mathbf{U}_k are all non-dominant and evenly distributed. Therefore, the set of N \mathbf{U}_k is the Pareto frontier of objection function (29), noted as \mathbf{PF}_k .

We assume that the DWC provider pursues the maximum profit within the grid impact limit (allowed maximum grid impact Λ_{max}) at k -th horizon, which is given below:

$$\mathbf{U}_k^* = \max_{\mathbf{X}_k} \{ \mathbf{PF}_k | \Lambda \leq \Lambda_{max} \}. \quad (31)$$

Therefore, the selection policy to find the decision variables from the Pareto frontier \mathbf{PF}_k is given below:

$$\mathbf{X}_k^* = \arg \max_{\mathbf{X}_k} \{ \mathbf{PF}_k | \Lambda \leq \Lambda_{max} \}. \quad (32)$$

Although it has been validated in Section V-B that this NSGA II is a suitable method for Pareto frontier exploration, it should be noticed that many other methods could be applied for this multi-objective optimization, such as Differential

TABLE III
CHARGING RATINGS AND PRICE OF DIFFERENT CHARGING SYSTEMS

Description	Notation	Value
Conductive charging [34] [35]		
Slow charging (3.7 kW)	C1	0.13 kWh/\$
Fast charging(7 kW)	C2	0.18 kWh/\$
Fast three-phase charging(22 kW)	C3	0.23 kWh/\$
Rapid charging(50 kW)	C4	0.31 kWh/\$
Ultra-rapid charging(150 kW)	C5	0.44 kWh/\$
Wireless charging		
DWC (80 kW)	C6	0.31-0.69 kWh/\$
Capital cost [21] [36] [37]		
Procurement price from AC grid	C_k^{grid}	0.13 ¹ 0.21 ² \$/KWh
Solar panel cost	C_{ren}	2250 \$/kW
Solar panel capacity	E_{solar}	25 MWh
DWC power track	C_{dwc}^p, C_{dwc}^c	500, 50 k\$/km
Storage cost	$C_{storage}$	145 \$/kWh
Storage capacity	$E_{storage}$	100 MWh
Maintenance cost	C_s	1.3 \$/MWh
Parameters of DWC model		
DWC power transfer efficiency	η_{dwc}	0.7
Length of DWC lane	L_{dwc}	50 km
Charging rating of DWC	P_{dwc}	80 kW
EV charging requirement (kWh)	$D_L - D_u$	0-50 kWh
Coefficient of (20)	α_1	3
Coefficient of (20)	α_2	0.3
Coefficient of (20)	β_0	1
Coefficient of (20)	β_1	5
Coefficient of (20)	β_2	10
Power transfer efficiency of storage	$\eta_s \eta'_s$	0.9
Grid limit	$< \Lambda_{max}$	0.16

1. Night (0.00am-5:00am) price. 2. Day price

Evolution, Particle Swarm Optimization, and Ant Colony Optimization.

B. Algorithm for multi-horizon optimization

For multi-horizon optimization, stochastic dynamic programming [33] based on tail policy is applied to solve (30). Based on the stochastic dynamic programming, the recursive process of (30) is presented as a Bellman equation:

$$\mathbf{F}_k = \max_{\mathbf{X}_k} \{ \mathbf{U}_k + \mathbf{F}_{k+1} \}. \quad (33)$$

The multiple horizon optimization is to solve the backward recursive process of (33) from K -th horizon to 1st horizon. In each horizon, \mathbf{X}_k^* is calculated via the multi-object optimization. Therefore, (30) is solved when the recursive process reaches to 1st horizon.

The full process of the stochastic dynamic programming is presented in Fig. 2. In each horizon, the model of DWC lane with storage and renewable energy is built based on Section II and III. The decision variables \mathbf{X}_k include the charging price p_k^{dwc} and electricity procurement d_k^{grid} . The outputs of the model are the profit and grid impact in the horizon. Besides the model of DWC system, the multi-objective optimization is enabled for finding the desired decision variables \mathbf{X}_k^* , which brings the maximum utility to the charging provider. The loop from last the horizon K to horizon 1 is carried out to achieve the multi-horizon optimization. Finally, the optimized profit and grid impact are carried out in each horizon and all horizons.

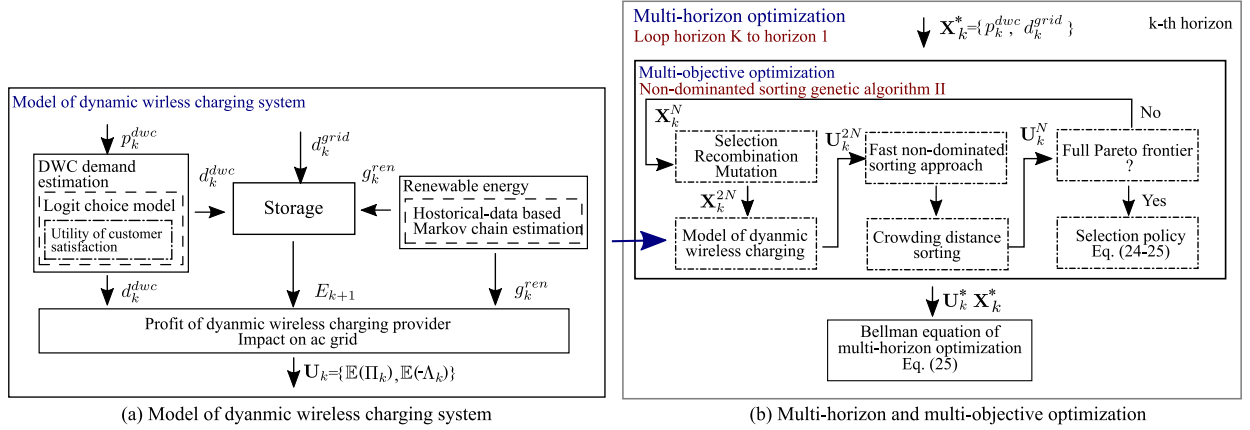


Fig. 2. Stochastic dynamic programming for formulation of optimization policy.

V. CASES STUDY

A full map of the transportation system and electricity grid is presented in Fig. 3. We assume that there are another 5 charging providers covering from slow charging to ultra-fast charging that are available for EVs except for DWC, denoted as C1-C6. A 50-km DWC lane (C6) is deployed on the highway. Storage units and solar panels are evenly deployed at every 12.5 km along with the DWC lane. IEEE 30-bus test case [38] is used as the AC grid to find out the grid impact from the DWC lane. Travel time $tt_a(f)$ on the highway is half of that on transportation routes at the same link flow.

The charging provider makes a profit from the revenue of DWC system and investigates the DWC lane, storage, and renewable energy generator. In a wholesale real-time electricity market, electricity is sold on an hourly basis. Therefore, our horizon economic analysis is conducted in each hour, and multi-horizon optimization repeats every $K=24$ horizons. The grid impact limit, which is the allowed maximum grid impact, is set at 0.16. The whole year's profit of the DWC lane covers the variance of renewable energy generation and car flow. The car flow data is collected from Highways England [39], which is drawn in Fig. 4. We assume that the car flow data can represent future EV flow data. Solar energy is used to represent renewable energy and its historical data is collected from National Grid [40]. We assume that 20% of EVs on the highway require charging. All the parameters of the DWC system are summarized in Table III.

The case studies are organised below. Results of DWC system model are presented in Section V-A including solar energy generation estimation and choice distribution among different charging providers. Section V-B shows the effectiveness of optimization policy for this DWC system to maximize the profit. Section V-C presents the economic of this DWC system via the daily profit performance and overall payback period.

A. Performance of developed DWC system model

1) *Solar power generation estimation:* We forecast the capacity factor of solar power, which is the ratio of energy generated over a horizon divided by the installed capacity, as it is convenient for comparing power generations among various

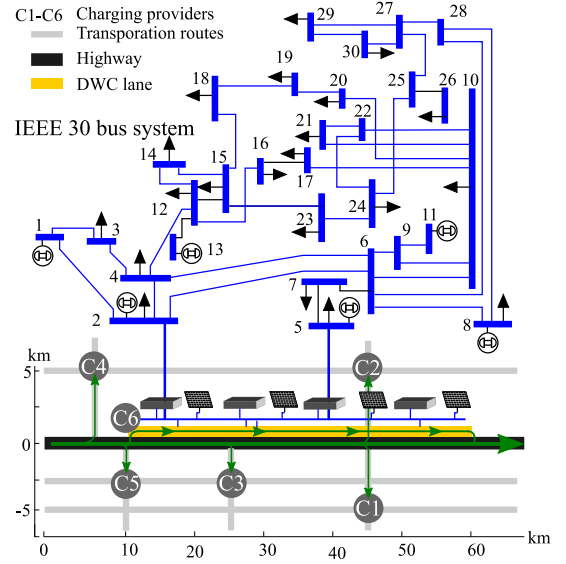


Fig. 3. Grid and transportation system with DWC lane

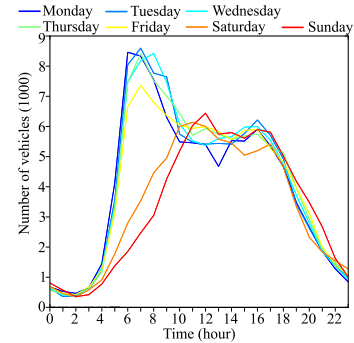


Fig. 4. Car flow of a week on M25 J12-13 highway

installed capacities. Then, capacity factors of solar power are divided into S states. And we define that every 5% of capacity factor is a state for the Markov Chain. The transition matrix \mathbf{TM}_k is estimated from the historical UK data [40] of solar power generation based on Section II-C.

By using derived \mathbf{TM}_k , solar energy generation based

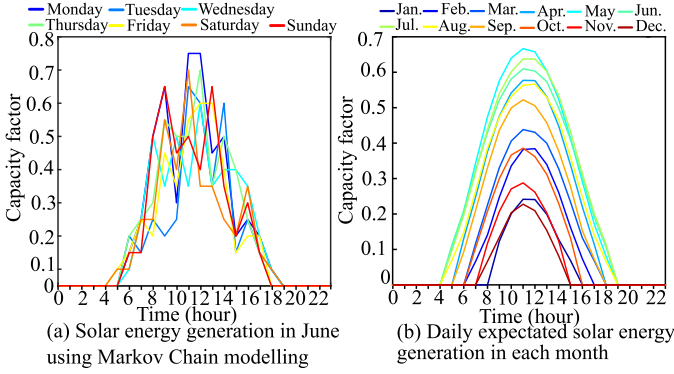


Fig. 5. Solar generation based on Markov chain modelling

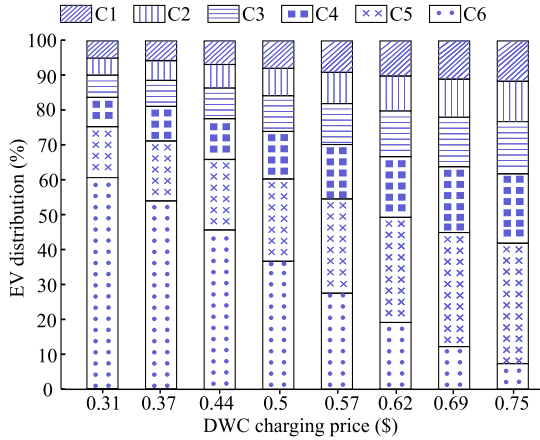


Fig. 6. Choice possibility under various DWC prices

Markov Chain modelling (4) is simulated. An example of one week's generation in June is shown in Fig. 5(a). It follows the trend of expected solar generation of June in Fig. 5(b) and inherits the random behaviour of historical solar generation thanks to the Markov Chain modelling. The overall yearly generation is shown in Fig. 5(b), which uses expectation value to present the overall trend of solar energy generation. It is found that solar panel generation reaches over 60% during 11:00-13:00 in May-July; while, the maximum generation in October-December is less than 30%, which will impose great pressure to the AC grid due to the massive electricity procurement from the DWC lane.

2) *Charging price impact on the choice among different charging types:* For the EVs on the highway requiring charging, 5 additional conductive types of charging providers are available in terms of charging price and charging speed, as shown in Table III. The choice possibility over these 6 charging technologies including DWC is developed via the logit model in Section II. How DWC pricing influences the EV charging choice is studied by changing the price from 0.31 to 0.75 \$ and results of choice possibility distribution are drawn in Fig. 6, where C6 is DWC and more details about charging types C1-C6 are given in Table III.

Overall, drivers are more willing to pick the chargers C4-C6 with high charging speed. Furthermore, it is found that DWC is more attractive if the charging price is below 0.57 \$/kWh.

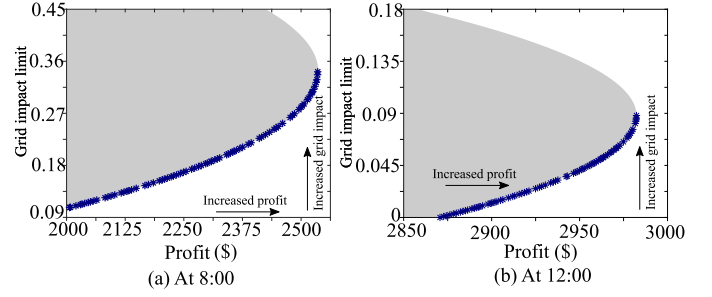


Fig. 7. Profit and grid impact Pareto frontier using NSGA2 on Monday December

As shown in Fig.6, the charging rating of DWC is smaller than ultra-rapid charging C5, more drivers still choose DWC even the charging prices are the same at 0.44 \$/kWh. DWC is not affordable at 0.75 \$/kWh for most of the drivers, which leads to less than 10% of drivers selecting DWC. It is found that DWC pricing has a significant influence on EV drivers' choices.

The highway integrated with the DWC lane has a large capacity for car flows. Travel time on this highway is not significantly delayed by a heavy EV flow. Our study suggests that further reducing the charging price of DWC attracts up to 60% EVs using DWC lane at 0.31 \$/kWh, as shown Fig. 6. However, price elasticity of the DWC lane in the urban area is different from that in the above situation. The urban route has lower car flow capacity and may cause a long travel time for the massive EV flow. For a DWC lane in the urban area, reducing its charging price may not effectively attract massive EVs due to the long travel time on urban routes. Furthermore, in that real urban traffic, it is needed to consider more factors such as traffic fluctuations and congestions, when modelling the travel time and estimating demand of DWC charging in Section III-B.

B. Performance of the optimization policy for DWC system

1) *Multi-objective optimization between profit and grid impact:* For presenting the multi-object optimization at each horizon, the trade-off between profit and grid impact at 8:00 and 12:00 of Monday December is drawn in Fig. 7. The typical daily solar generation of December and car flow on Monday, as shown in Fig. 4 and 5, are used for validating the optimization. As shown in Fig. 7, the grey area is all possible values of profit and grid impact calculated from the full range of DWC price and electricity procurement. Its Pareto frontier is accurately tracked by the proposed NSGA2 algorithm, as shown in both Fig. 7(a) and Fig. 7(b) (blue dots). It is found obviously that the higher profit results in severer grid impacts along their Pareto frontier.

Based on the proposed policy function (31-32), maximized profit points on the Pareto frontier are tracked within various impact grid limits. By comparing Fig. 4 and 5, it is also found that the grid impact at 8:00 is comparatively larger than that at 12:00 with the similar maximized profit. As the solar panel generates insufficient energy for the peak flow in the morning, the demand for electricity procurement increases, which imposes a higher burden on the grid.

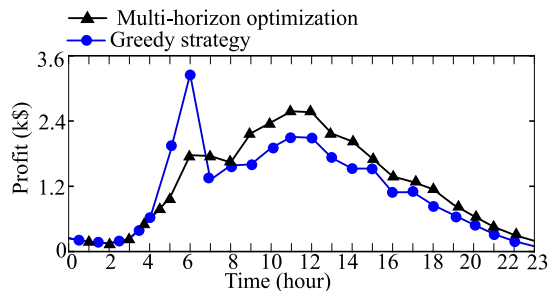


Fig. 8. Comparison between multi-horizon optimization using stochastic dynamic programming and greedy strategy

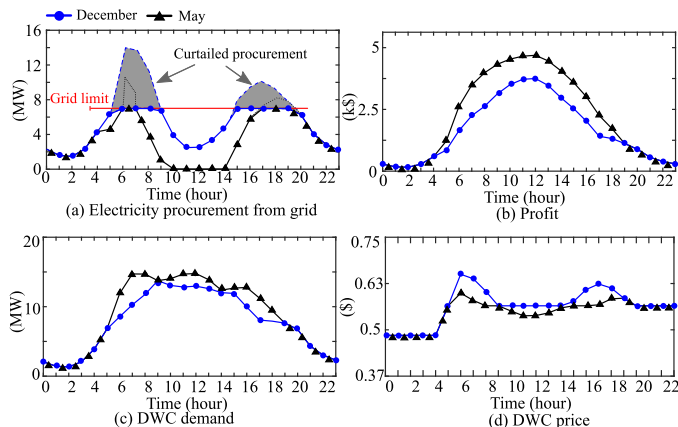


Fig. 9. Impact of December's and May's solar generation on the DWC system

2) *Multi-horizon optimization validation*: The advance of multi-horizon optimization strategy is presented by comparing to the greedy strategy, which maximizes the profit of the current horizon without considering the future. The multi-horizon optimization strategy uses a stochastic dynamic programming algorithm as explained in Section IV-B. Both strategies use the same multi-object optimization and their results are shown in Fig. 8. It is found that the greedy strategy earns more profit at an early stage of the day and less profit after 7:00 am. This is because that the stored electricity is oversupplied during the EV peak time in the morning by greedy strategy without considering the remaining hours. The total daily profit made by multi-horizon optimization strategy and greedy strategy is, respectively, 30,661 \$ and 27781 \$. The multi-horizon optimization strategy makes more daily profit because it exploits the information of the whole day including generation estimation of renewable energy and EV demand estimation. Accordingly, the stored electricity is well distributed to maximize the daily profit.

C. Economic performance of the dynamic wireless charging system

1) *Daily profit performance of the dynamic wireless charging system with difference solar generation*: Solar generation varies significantly among different months especially between December and May, as shown in Fig. 5. Their solar generation impacts on DWC system are compared and the results are shown in Fig. 9. The insufficient electricity supply from solar

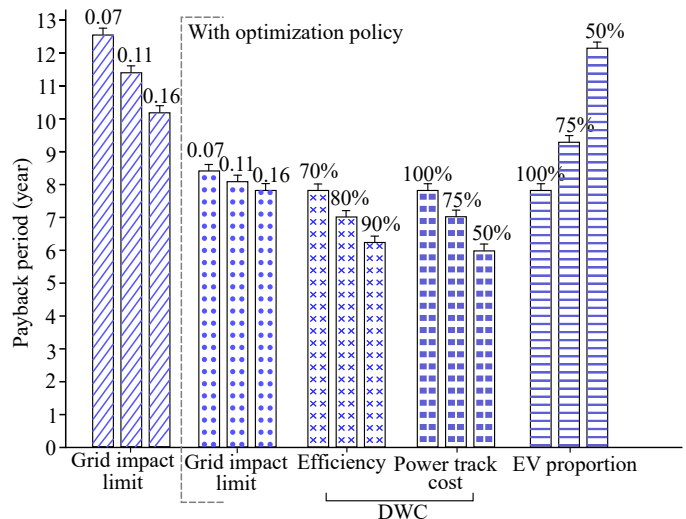


Fig. 10. Payback period under various factors.

TABLE IV
DETAILED VALUES OF PAYBACK PERIOD UNDER VARIOUS FACTORS

Factor		Payback period (Year)	
No optimization policy	Grid impact limit	0.16	10.1
		0.11	11.4
		0.07	12.5
With optimization policy	Grid impact limit	0.16	7.9
		0.11	8.1
		0.07	8.4
	DWC power transfer efficiency	70%	7.9
		80%	7.0
		90%	6.5
	DWC power track cost	100%	7.9
		75%	7.1
		50%	6.3
	EV proportion	100%	7.9
75%		9.3	
		50%	12.1

panels in December, as shown in Fig. 5, makes the DWC system procuring more electricity from the grid. However, a large portion of electricity procurement is curtailed to maintain the grid impact within the proposed limit of 0.16, as shown in Fig 9 (a). Therefore, the DWC system makes less profit from 5:00 to 19:00 in December due to its insufficient solar energy supply and grid impact limit, as shown in Fig. 9 (b). The total aggregated daily profit in December is much lower than that of May, which are respectively 30,660 \$ and 53,486 \$. The same Monday EV flows are applied in December and May respectively. It is found that more DWC demand of May is regulated from 5:00 to 19:00 by the DWC optimization policy to make more profit because of a larger amount of solar energy generation in May, as shown in Fig. 9 (c). For attracting more DWC demand in May, its DWC price, which is regulated by the DWC optimization policy, is lower than the price of December, as shown in Fig. 9 (d).

2) *Sensitive analysis for payback period*: Various factors including grid impact limit, DWC efficiency, DWC power track cost, and EV proportion are analyzed to identify their contribution to the payback period of the overall DWC system, and the results are presented in Fig. 10 or in Table IV. The payback period is calculated based on the yearly profit of the DWC system, which covers the variance of weekly EV

flow (Fig. 4) and monthly solar generation (Fig. 5). If no optimization policy is applied, the charging price is fixed at 0.5 \$/kWh.

When a grid impact limit of 0.16 is applied, the payback period without optimization policy is 10.1 years, while it is shortened to 8 years by using optimization policy as shown in Fig. 10 or Table IV. Moreover, as the grid impact limit is tightened to 0.07, the payback period without optimization policy increases by 20%, while the payback period with optimized strategy only rises by 4%. EVs would be gradually dominant in the future vehicle market, it is well worth finding out how the increasing EV proportions affect the economics of the DWC system. The results of this relevant economic analysis are shown in Fig. 10 and Table IV. It is found that when the EV proportion increases from 50% to 100%, the payback period is shortened from 12.1 years to 7.9 years. In Fig. 10, we can also see that when the efficiency of DWC improves to 90%, the payback period is shortened from 7.9 to 6.5 years. Also, as the cost of DWC cuts to 50%, the payback period is reduced to 6.3 years.

VI. CONCLUSION

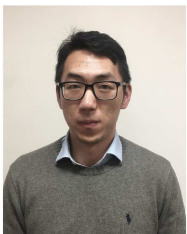
A comprehensive framework to evaluate the economic viability for the DWC system, including a DWC lane, renewable integration, and storage system, has been proposed and validated in this paper. It is shown via the proposed choice model that EV drivers prefer the quick charging speed if the charging price is below 0.56 \$/kWh. Within this charging price range, the DWC is more attractive over conductive charging because of its capability of non-stop charging. It has been validated that the proposed multi-objective optimization policy can track the Pareto frontier of the DWC profit and the grid impact accurately. Moreover, more solar generation helps to produce the higher profit of the DWC system. For example, compared to December, daily profit in May is 180% higher.

With the multi-objective and multi-horizon optimization policy, the payback period is around 8 years, while it is 10.1 years with a fixed charging price strategy. By using this optimization policy, the tight grid impact limit does not have a significant impact on postponing the payback period such as 4%, while the DWC system with a fixed charging price strategy requires 20% postponing the payback period. If the efficiency and the cost of the DWC lane respectively increase to 90% and reduce to 50%, the payback period is shortened to 6.5 years and 6.3 years.

REFERENCES

- [1] Programme on Climate and Energy, "International trade governance and sustainable transport: The expansion of electric vehicles." International Centre for Trade and Sustainable Development, December 2017. [Online]. Available: <https://www.ictsd.org/sites/default/files/research/international-trade-governance-and-sustainable-transport-mahesh-sugathan.pdf>.
- [2] M. Fuller, "Wireless charging in california: Range, recharge, and vehicle electrification," *Transportation Research Part C journal*, vol. 67, pp. 343–356, 2016.
- [3] Zhibin, Chen, W. Liu, and Y. Yin, "Deployment of stationary and dynamic charging infrastructure for electric vehicles along traffic corridors," *Transportation Research Part C journal*, vol. 77, pp. 185–206, 2017.
- [4] J. Huh, S. W. Lee, W. Y. Lee, G. H. Cho, and C. T. Rim, "Narrow-width inductive power transfer system for online electrical vehicles," *IEEE Transactions on Power Electronics*, vol. 26, no. 12, pp. 3666–3679, 2011.
- [5] G. Buja, M. Bertoluzzo, and H. K. Dashora, "Lumped track layout design for dynamic wireless charging of electric vehicles," *IEEE Transactions on Industrial Electronics*, vol. 63, no. 10, pp. 6631–6640, 2016.
- [6] C. Park, S. Lee, S. Y. Jeong, G. Cho, and C. T. Rim, "Uniform power i-type inductive power transfer system with dq-power supply rails for on-line electric vehicles," *IEEE Transactions on Power Electronics*, vol. 30, no. 11, pp. 6446–6455, 2015.
- [7] L. Chen, G. R. Nagendra, J. T. Boys, and G. A. Covic, "Double-coupled systems for ipt roadway applications," *IEEE Journal of Emerging and Selected Topics in Power Electronics*, vol. 3, no. 1, pp. 37–49, 2015.
- [8] Z. Wang, S. Cui, S. Han, K. Song, C. Zhu, M. I. Matveevich, and O. S. Yurievich, "A novel magnetic coupling mechanism for dynamic wireless charging system for electric vehicles," *IEEE Transactions on Vehicular Technology*, vol. 67, no. 1, pp. 124–133, 2018.
- [9] A. N. Azad, A. Echols, V. A. Kulyukin, R. Zane, and Z. Pantic, "Analysis, optimization, and demonstration of a vehicular detection system intended for dynamic wireless charging applications," *IEEE Transactions on Transportation Electrification*, vol. 5, no. 1, pp. 147–161, 2019.
- [10] X. Dai, J. Jiang, and J. Wu, "Charging area determining and power enhancement method for multiexcitation unit configuration of wirelessly dynamic charging ev system," *IEEE Transactions on Industrial Electronics*, vol. 66, no. 5, pp. 4086–4096, 2019.
- [11] Q. Zhu, L. Wang, Y. Guo, C. Liao, and F. Li, "Applying lcc compensation network to dynamic wireless ev charging system," *IEEE Transactions on Industrial Electronics*, vol. 63, no. 10, pp. 6557–6567, 2016.
- [12] H. Feng, T. Cai, S. Duan, J. Zhao, X. Zhang, and C. Chen, "An lcc-compensated resonant converter optimized for robust reaction to large coupling variation in dynamic wireless power transfer," *IEEE Transactions on Industrial Electronics*, vol. 63, no. 10, pp. 6591–6601, 2016.
- [13] S. Y. Choi, B. W. Gu, S. Y. Jeong, and C. T. Rim, "Advances in wireless power transfer systems for roadway-powered electric vehicles," *IEEE Journal of Emerging and Selected Topics in Power Electronics*, vol. 3, no. 1, pp. 18–36, 2015.
- [14] C. C. Mi, G. Buja, S. Y. Choi, and C. T. Rim, "Modern advances in wireless power transfer systems for roadway powered electric vehicles," *IEEE Transactions on Industrial Electronics*, vol. 63, no. 10, pp. 6533–6545, 2016.
- [15] S. Laporte, G. Coquery, V. Deniau, A. D. Bernardinis, and N. Hautiere, "Dynamic wireless power transfer charging infrastructure for future evs: From experimental track to real circulated roads demonstrations," *World Electric Vehicle Journal*, vol. 10, no. 84, pp. 1–22, 2019.
- [16] T. A. Nergaard and J. B. Straubel, "Integrated inductive and conductive electrical charging system," U.S. Patent US8933661B2, Jan. 2015.
- [17] M. Sheng, A. V. Sreenivasan, B. Sharp, D. Wilson, and P. Ranjitkar, "Economic analysis of dynamic inductive power transfer roadway charging system under public-private partnership—evidence from new zealand," *Technological & Forecasting Social Change*, vol. 154, pp. 1–10, 2020.
- [18] A. Shekhar, V. Prasanth, P. Bauer, and M. Bolech, "Economic viability study of an on-road wireless charging system with a generic driving range estimation method," *energies*, vol. 9, no. 17, pp. 1–20, 2016.
- [19] Y. D. Ko and Y. J. Jang, "The optimal system design of the online electric vehicle utilizing wireless power transmission technology," *IEEE Transactions on Intelligent Transportation Systems*, vol. 14, no. 3, pp. 1255–1265, 2013.
- [20] Y. D. Ko, Y. J. Jang, and M. S. Lee, "The optimal economic design of the wireless powered intelligent transportation system using genetic algorithm considering nonlinear cost function," *Computers & Industrial Engineering*, vol. 89, pp. 67–79, 2015.
- [21] S. Jeong, Y. J. Jang, and D. Kum, "Economic analysis of the dynamic charging electric vehicle," *IEEE Transactions on Power Electronics*, vol. 30, no. 11, pp. 6368–6377, 2015.
- [22] I. Hwang, Y. J. Jang, Y. D. Ko, and M. S. Lee, "System optimization for dynamic wireless charging electric vehicles operating in a multiple-route environment," *IEEE transactions on Intelligent Transportation System*, vol. 19, no. 6, pp. 1709–1726, 2018.
- [23] C. A. García-Vázquez, F. Llorens-Iborra, L. M. Fernández-Ramírez, H. Sánchez-Sainz, and F. Jurado, "Comparative study of dynamic wireless charging of electric vehicles in motorway, highway and urban stretches," *Energy*, vol. 137, pp. 42–57, 2017.

- [24] T. Kan, F. Lu, T. Nguyen, P. P. Mercier, and C. C. Mi, "Integrated coil design for ev wireless charging systems using lcc compensation topology," *IEEE Transactions on Power Electronics*, vol. 33, no. 11, pp. 9231–9241, 2018.
- [25] E. Namor, F. Sossan, R. Cherkaoui, and M. Paolone, "Control of battery storage systems for the simultaneous provision of multiple services," *IEEE Transactions on Smart Grid*, vol. 10, no. 3, pp. 2799–2808, 2019.
- [26] J. Shen, S. Dusmez, and A. Khaligh, "Optimization of sizing and battery cycle life in battery/ultracapacitor hybrid energy storage systems for electric vehicle applications," *IEEE Transactions on Industrial Informatics*, vol. 10, no. 4, pp. 2112–2121, 2014.
- [27] K. Train, *Discrete Choice Methods with Simulation*. Cambridge, U.K.: Cambridge University Press, 2 ed., 2009.
- [28] Z. Guo, Z. Zhou, and Y. Zhou, "Impacts of integrating topology reconfiguration and vehicle-to-grid technologies on distribution system operation," *IEEE Transactions on Sustainable Energy*, vol. 11, no. 2, pp. 1023–1032, 2020.
- [29] Y. SHEFFI, *Urban Transportation Networks*. Englewood Cliffs, N.J. 07632, U.S.A.: Prentice-Hall, Inc., 1 ed., 1985.
- [30] L. Wang, A. H. C. Ng, and K. Deb, *Multi-objective Evolutionary Optimisation for Product Design and Manufacturing*. London, U.K.: Springer-Verlag London, 1 ed., 2011.
- [31] K. Deb, A. Pratap, S. Agarwal, and T. Meyarivan, "A fast and elitist multiobjective genetic algorithm: Nsga-ii," *IEEE Transactions on Evolutionary Computation*, vol. 6, no. 2, pp. 182–197, 2002.
- [32] N. Srinivas and K. Deb, "Multiobjective optimization using nondominated sorting in genetic algorithms," *Journal of Evolutionary Computation*, vol. 2, no. 3, pp. 221–248, 1995.
- [33] D. P. BERTSEKAS, *Dynamic Programming and Optimal Control*. Nashua, New Hampshire, U.S.A.: Athena Scientific, 3 ed., 2012.
- [34] Pod Point, "How long does it take to charge an electric car?." [Online]. Available: <https://pod-point.com/guides/driver/how-long-to-charge-an-electric-car>.
- [35] Polar network, "How much does the polar network cost?." Zap Map. [Online]. Available: <https://www.zap-map.com/charge-points/public-charging-point-networks/polar-network/>.
- [36] Chris Lilly, "Ev energy tariffs." Zap Map. [Online]. Available: <https://www.zap-map.com/charge-points/ev-energy-tariffs/>.
- [37] IRENA, "Electricity storage and renewables: Costs and markets to 2030," tech. rep., International Renewable Energy Agency, Abu Dhabi, United Arab Emirates, Tech. Rep., 2017.
- [38] I. Dabbaghi and R. Christie, "30 Bus Power Flow Test Case." [Online]. Available: <https://icseg.iti.illinois.edu/power-cases/>.
- [39] Highways England, "Traffic flow data." Highways England. [Online]. Available: <http://tris.highwaysengland.co.uk/detail/trafficflowdata>.
- [40] Sheffield Solar and National Grid, "PV generation in the UK." The University of Sheffield Microgen. [Online]. Available: <https://www.solar.sheffield.ac.uk/pvlive/#>.



Chuanyue Li (M'17) received the B.Eng. degrees from both Cardiff University, UK and North China Electric Power University, China, in 2013 and the Ph.D. degree from Cardiff University, UK, in 2017. In 2018, he was a post-doc at the Laboratory of Electrical Engineering and Power Electronics (L2EP), Lille, France. Currently, He is a Research Associate at the School of Engineering, Cardiff University, Wales, UK. His research interests include HVDC control and protection, power electronics.



Xue Dong received the Ph.D. degree from Cardiff University, Cardiff, UK, in 2018. From 2018 to 2021, she was a research assistant for Julian Hodge Institute of Applied Macroeconomics at Cardiff University. Currently, she is a Lecturer at the School of Economics, Zhejiang University of Finance and Economics, Hangzhou, China. Her research interests include applied macroeconomics, and energy economics.



Liana M. Cipcigan (M'08) is a Professor at Cardiff University's School of Engineering leading Sustainable Transport cross-cutting theme. She is Director of the Electric Vehicle Centre of Excellence and leader of Transport Futures Research Network. She was at the forefront of the shift to electrified transport for over a decade being recognised nationally and internationally as an expert in EVs and Smart Grids leading the £1M EPSRC Network+ "Decarbonising Transport through Electrification (DTE), a Whole system approach". She has collaborated

widely with industry, more recently during her secondment at National Grid under Royal Academy of Engineering Industrial Fellowship, working in the Energy Insights department responsible for the Future Energy Scenarios. She has held as PI and Co-I grants in the excess of £6.5M from EPSRC, Royal Academy of Engineering, Innovate UK, UKERC, Welsh European Funding Office, EU FP7/H2020 and industry.



Manu A. Haddad (Member, IEEE) received the degree in electrical engineering and the Ph.D. degree in high-voltage engineering from Cardiff University, Cardiff, U.K., in 1985 and 1990, respectively.

He is currently a Professor with Cardiff University. He has published an IET-Power Series Book on "Advances in High Voltage Engineering (IET, 2004)." His research interests include overvoltage protection, insulation systems, insulation coordination, and earthing systems.

Prof. Haddad is a member of CIGRE working groups, BSI PEL1/2, and IEC ACTAD committee. He is a fellow of the IET and the Learned Society of Wales. He serves on the scientific committees for several international conferences. He is also the Chair of IEC TC37.



Mingyu Sun (M'14) received the B.Eng. degree in electrical engineering from Shandong University, Jinan, China, in 2013, and the M.Sc. and Ph.D. degrees in electrical power engineering from The University of Manchester, Manchester, U.K., in 2014 and 2020, respectively. From Sept 2019 to August 2021, he was an innovation engineer with National Grid Electricity Transmission, U.K. He is currently a senior engineer with National Grid ESO, U.K. His research interests include applications of power electronics in power systems, and wide-area monitoring,

protection, and control systems.



Jun Liang (M'02-SM'12) received the B.Sc. degree from Huazhong University of Science and Technology, Wuhan, China, in 1992 and the M.Sc. and Ph.D. degrees from the China Electric Power Research Institute (CEPRI), Beijing, in 1995 and 1998, respectively. From 1998 to 2001, he was a Senior Engineer with CEPRI. From 2001 to 2005, he was a Research Associate with Imperial College London, U.K.. From 2005 to 2007, he was with the University of Glamorgan as a Senior Lecturer. Currently, he is a Professor at the School of Engineering, Cardiff

University, Cardiff, U.K.. He is a Fellow of the Institution of Engineering and Technology (IET). He is the Chair of IEEE UK and Ireland Power Electronics Chapter. He is an Editorial Board Member of CSEE JPES. He is the Coordinator and Scientist-in-Charge of two EC Marie-Curie Action ITN/ETN projects: MEDOW (€3.9M) and InnoDC (€3.9M). His research interests include HVDC, MVDC, FACTS, power system stability control, power electronics, and renewable power generation.



Wenlong Ming (M'16) received the B.Eng. and M.Eng. Degrees in Automation from Shandong University, Jinan, China, in 2007 and 2010, respectively. He received the Ph.D. degree in Automatic Control and Systems Engineering from the University of Sheffield, Sheffield, U.K., in 2015. He was the winner of the prestigious IET Control & Automation Doctoral Dissertation Prize in 2017. He has been a Lecturer of Power Electronics at Cardiff University, U.K., since August 2016 and a Senior Research Fellow funded by Compound Semiconductor Applications (CSA) Catapult, U.K., for 5 years since April 2020.

He was with the Center for Power Electronics Systems (CPES), Virginia Tech, Blacksburg, USA in 2012 as an academic visiting scholar. He has (co-)authored more than 50 papers published in leading journals or refereed IEEE conferences. His research interests focus on Medium Voltage DC systems for electricity distribution networks and characterisation, modelling, applications of wide-bandgap compound semiconductors.